Bachelor Thesis

Permanent Magnet Particle Traps

Author:
Sam Herz *(S4463978)*

Supervisor:
Dr. Steven A. Jones
Second Examiner:
Dr. Kristof A. M. de Bruyn

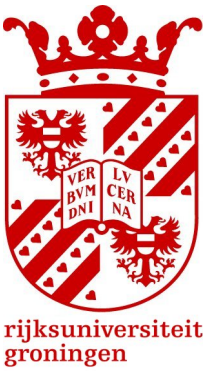

DiCE Group
Faculty of Science and Engineering
University of Groningen
Groningen, the Netherlands

July 11, 2023

Permanent Magnet Particle Traps

Sam Herz

Abstract

Comparisons of trapped anti-hydrogen atoms and hydrogen atoms promise to test nature's fundamental symmetries such as the charge conjugation parity time reversal (CPT) theorem. To be able to form and trap (anti-)hydrogen particles, nested Penning-Ioffe traps are used, which is a superposition of a Penning trap, responsible for trapping charged particles, and a magnetic Ioffe trap, responsible for confining neutral (anti-)hydrogen particles. Conventional, Ioffe traps, used at facilities such as ALPHA and ATRAP, constitute of superconducting wires and need to be cryogenically cooled. The aim of this research was to investigate whether it is possible to design an Ioffe trap, exclusively out of N52 (sintered NdFeB) magnets, which can trap (anti-)hydrogen particles. Using Comsol Multiphysics 6.0 software, magnetic flux density studies were conducted on three potential design models. It was found that for all models, it is possible to create a three-dimensional static magnetic minimum inside the traps with trap depth values ranging from 0.04K up to 0.21K. The research conducted in this paper is yet to be experimentally verified but suggests the possibility of constructing a cost-friendly alternative to conventional neutral traps.

Acknowledgements

Firstly, I would like to thank my supervisor Dr. S.A. Jones for his guidance, support and dedication.
In addition, I would like to thank Nikos Efthymiadis, Tom Sonius and Joël Zwart for the amazing companionship I experienced during my time working on this project. It was truly an exceptional experience to be a part of such a dynamic group.

Contents

1 Introduction

In the last decade, creating and especially trapping anti-hydrogen has improved drastically to the point that more than 1000 atoms can be simultaneously trapped [1]. Comparing anti-hydrogen with hydrogen enables to better understand matter-antimatter symmetries such as CPT (charge-parity-time) invariance and the weak equivalence principle while investigating the gravitational behaviour of anti-hydrogen [2]. To be able to synthesize and trap anti-hydrogen in the first place, a nested Penning-Ioffe trap is used [3]. It is a superposition of a Penning trap, to trap charged positron and anti-proton, and an Ioffe trap, to trap neutral anti-hydrogen [3]. Penning-Ioffe traps constructed at ALPHA and ATRAP (Anti-hydrogen trap) were able to successfully trap anti-hydrogen since 2002 and 2012 respectively [4][5].

The idea of an Ioffe trap is to trap neutral particles by generating a constant magnetic field minimum inside the trap. Neutral particles such as anti-hydrogen only interact with magnetic fields via their magnet dipole moment [6]. Due to the fact that the dipole moment of anti-hydrogen is relatively small, high currents are needed as a result. The best solution nowadays is to use superconducting wires in the magnets which only operate at low temperatures and are placed in liquid helium at 4.2 Kelvin (-268°C) [6]. Using superconductors provides advantages such that the magnetic field can be changed by applying different currents through the wires thus being more controllable. However, the concept of Ioffe traps is limited by the fact that superconductors need to operate at very low temperatures which brings financial and geometrical setup limitations along it. This problematic gives raise to the research question of this report whether it is possible to design an Ioffe trap, exclusively out of permanent magnets, which is strong enough to trap (anti-)hydrogen particles. By using the multiphysics software COMSOL, different models will be modeled. Using magnetic flux density studies it will be investigated whether it is possible to successfully construct a closed magnetic minimum inside such a trap or not. In the same way as an conventional Ioffe trap, there will be two parts. A n-pole part, quadrupole, to confine the particle radially and a part to close the trap axially. Ioffe traps are of interest as confining neutral particles represents a higher challenge compared to trapping charged particles. In addition, an Ioffe trap can be combined with different charged traps such as Penning or Radio-frequency traps, to give only a few examples.

2 Theorical Overview

2.1 Penning trap

Charged particles, such as positron and anti-proton, interact with magnetic and electric fields. Intuitively, the best way to trap these particles would be to create a three-dimensional electrostatic potential minimum. In this minimum, a force directs the particles toward the center of the trap from all directions. However, according to Earnshaw's theorem, electrostatic fields can only trap particles at most along two axes [7][8]. To be more precise, for a charged particle, a three-dimensional quadrupolar potential ϕ is responsible for creating an electrostatic field $\boldsymbol{E} = -\boldsymbol{\nabla}\phi$ which represents not only an axial harmonic potential well but also a radial repulsive potential [8]. Hence, not confining the particle radially. This situation is best illustrated using Fig.1. However, by introducing a uniform magnetic field B, the motion of the particle is confined along the radial direction thus enabling to form a stable 3D trap [7].

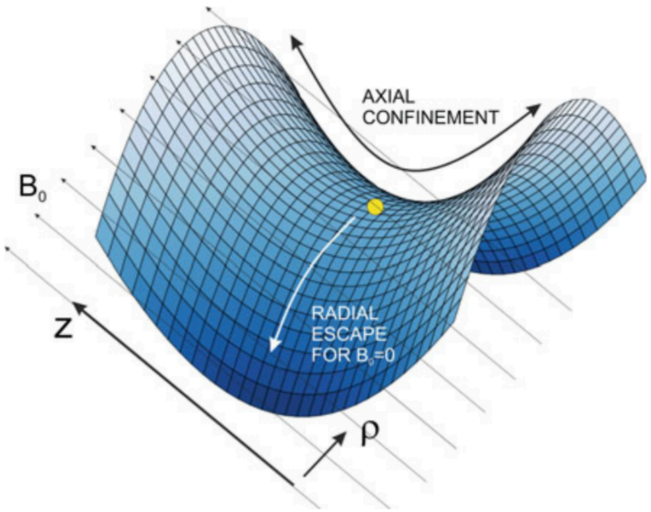

Figure 1: Illustration of the electrostatic potential saddle created inside a Penning trap, in the absence of a magnetic field B_0, where z is along the axial axis and ρ along the radial axis. Image from [8].

An example of a stable 3D charge trap is the Penning trap. Electrodes produce the static electrostatic field E which confines particles axially, along the trap axis, and a constant parallel magnetic field confines radially [4][7]. An ideal Penning trap would consist of at least three hyperbolically shaped electrodes that create a perfect quadratic electric field [4][7]. In reality a simplified version, the so-called Penning-Malmberg trap is used which consists of cylindrical shaped electrodes [4].

The resulting equation of motion for charged particles trapped in a penning trap follows the Lorentz force

$$\boldsymbol{F} = q(-\boldsymbol{\nabla}\phi + \boldsymbol{v} \times \boldsymbol{B}) = q(\boldsymbol{E} + \boldsymbol{v} \times \boldsymbol{B}) \tag{1}$$

where q is the charge of the particle, ϕ is the electrostatic potential, E is the electric field, v is the particle's velocity and B the magnetic field [4][7].

2.2 Ioffe trap

Neutral particles such as hydrogen and anti-hydrogen are not affected by electric fields but only interact with magnetic fields via their magnet dipole moment μ [6]. In this case, the neutral particles need to be trapped in a three-dimensional magnetic field minimum which can be achieved by using an Ioffe trap [7]. The particle's magnetic moment needs to be aligned anti-parallel to the magnetic field of the trap to be attracted towards the magnetic field minimum [2]. As (anti-)hydrogen atoms have hyperfine states which are diamagnetic, they provide this requirement. An Ioffe trap is made of two parts. 2n current wires are placed circularly along the axis of confinement. By alternating the direction of the current of each wire opposite to its neighbour, an n-pole magnet is established where n = 4,6,8, etc [2][3]. The most common configurations are quadrupole (n = 4) and octupole (n = 8) configurations. In the case of a quadrupole configuration, the trap is also referred to as a Pritchard-Ioffe trap [3]. To confine the particles radially, two current loops, so-called mirror coils, are placed perpendicular to the n-pole configuration. As seen in Fig.2, they are separated from each other by a large distance compared to their diameter, and the current runs in the same direction for both coils [3].

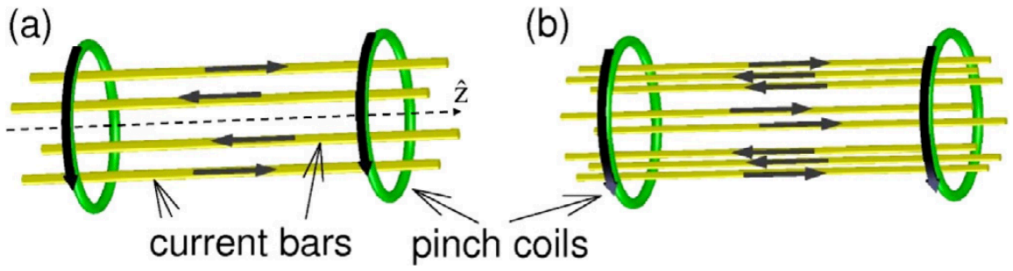

Figure 2: Illustration of a conventional Ioffe trap with a quadrupole (a) and octupole configuration (b) using vertical current bars. Two mirror coils, pinch coils, are used to confine the trap radially. Image from [3].

For the particles, such as anti-hydrogen, to be confined inside an Ioffe trap, it is important to evaluate the trap depth. The trap depth gives important insights into the maximum kinetic energy of a neutral particle to stay trapped in the magnetic field minimum of the trap. As previously mentioned, only particles possessing a magnetic moment μ are in the first place eligible to be trapped. The magnetic moment for a ground state (anti-)hydrogen particle is similar to 1 Bohr magneton μ_B [7] [8]. The Bohr magneton is defined as $\mu_B = \frac{e\hbar}{2m_e} \approx 9.274 \times 10^{-24} \frac{J}{T}$ where e is the elementary charge, $\hbar$ is the reduced Planck's constant and m_e is the electron rest mass [8]. As a result, the potential energy U of (anti-)hydrogen with magnetic moment μ_B in a magnetic field B is

$$U = -\boldsymbol{\mu_B} \cdot \boldsymbol{B} \tag{2}$$

The minus sign appears as (anti-)hydrogen atoms have hyperfine states which are diamagnetic. From equation 2, it can be concluded that the particles have a minimum energy at low magnetic fields thus explaining why they are attracted towards the magnetic minimum. In order to identify the trap depth, it is not enough to know only the overall magnetic field strength B of the trap. The region with the highest measured field $|B|_{Wall}$, next to the walls of the traps, and the region with the lowest field $|B|_{Center}$, in the central magnetic minimum, need to be

compared [2]. Meaning that the theoretical maximum kinetic energy K_{max} for a particle inside a magnetic trap is equivalent to the trap depth W value. For a particle to be trapped inside the magnetic minimum, its kinetic energy value K needs to be below W. As a result, the trap depth is defined as followed

$$W = K_{max} = -U = \boldsymbol{\mu_B}(|\boldsymbol{B}|_{Wall} - |\boldsymbol{B}|_{Center}) \tag{3}$$

The relation $K_{max} = -U$ follows from the principle of energy conservation. To be able to express the trap depth W in Kelvin, equation 3 is divided by the Boltzmann constant $k_B \approx 1.380 \times 10^{-23} \frac{J}{K}$ [9].

$$W = \frac{\boldsymbol{\mu_B}(|\boldsymbol{B}|_{Wall} - |\boldsymbol{B}|_{Center})}{k_B} \tag{4}$$

2.3 Nested Penning trap

To be able to produce and capture (anti-)hydrogen, a nested Penning-Ioffe trap is required. A nested Penning-Ioffe trap is a superposition of a Penning trap, to trap positron/electrons and (anti-)protons, and an Ioffe trap, which is responsible to trap (anti-)hydrogen. To trap (anti-)hydrogen atoms, the superimposed Ioffe trap needs to be active, which means creating a 3D magnetic minimum, before (anti-)hydrogen is formed in the first place [3][7]. However, the magnetic field created by the Ioffe trap perturbs the homogeneous magnetic field needed for the Penning trap. Resulting in the loss of (anti-)protons and positrons/electrons away from the central axis. Fig.3 shows how the field lines of the magnetic field of a Penning trap are distorted by superimposing a multipole on top of it. As shown in Fig.3, the magnetic field lines converge radially in one axial direction and diverge in the other when a multipole is introduced. If the B-field of the multipole is strong enough, the charged particles will end up in the walls of the nested Penning-Ioffe trap as their trajectory follows the field lines.

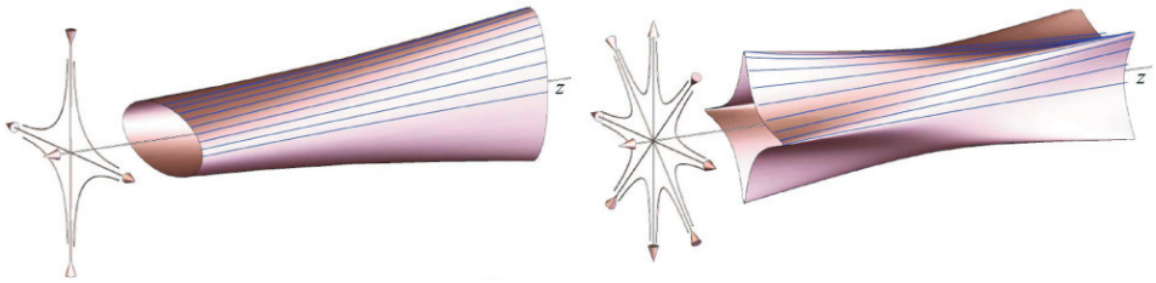

Figure 3: Magnetic field lines for a quadrupole (left) and octupole (right) when superimposed on a homogeneous magnetic field created by a Penning trap. Image from [7].

This introduces the parameter of critical radius r_{crit}, which represents the maximal radius behind which all charged particles are directed into the trap walls by the radial field of the Ioffe trap [3][7]. For a quadrupole, the critical radius is expressed as

$$r_{crit} = R_w \exp\left(-\frac{1}{2}\frac{B_w}{B_z}\frac{L}{R_w}\right) \tag{5}$$

and for a octupole it is

$$r_{crit} = \frac{R_w}{\sqrt{1 + \frac{B_w}{B_z}\frac{L}{R_w}}} \tag{6}$$

where R_w is the wall radius, B_w the multipole field at the wall, B_z the axial magnetic field and L the axial path length [7]. Using Fig.4 and the equations 5 and 6, it is observed that for higher-order multipoles, the magnetic field of the trap varies stronger with the radius, resulting in a larger critical radius. In other words, the field created by an octupole configuration is less, near the trap axis, compared to the quadrupole field, reducing the loss of charged particles.

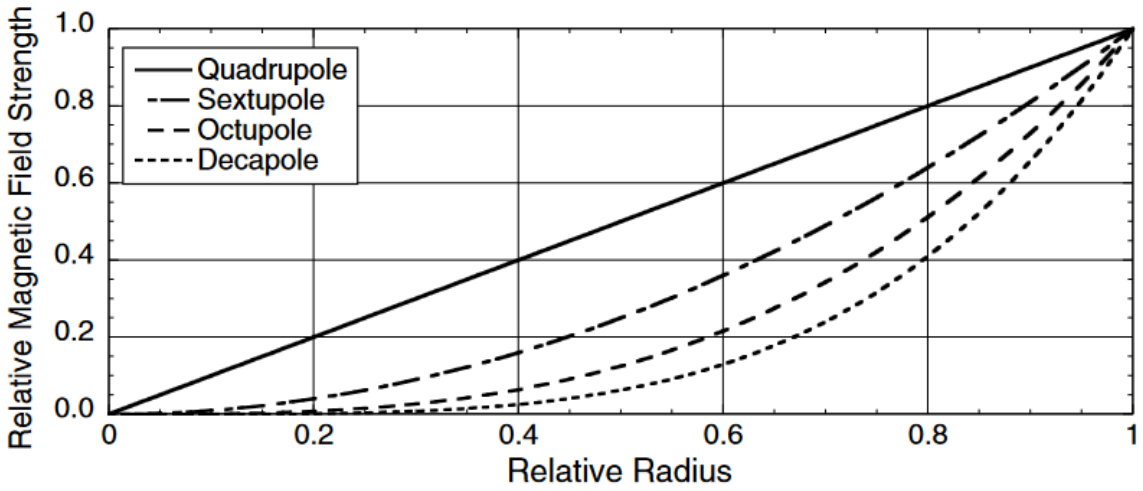

Figure 4: Graph of the relative magnetic field strength from different multipoles with respect to the relative radius. The data is normalized so that all multipoles have a magnetic field strength of one at the wall which is located at a radius one. Image from [7].

2.4 Breit-Rabi diagram

In order to understand whether (anti-)hydrogen particles can be trapped in a static magnetic field or not, the structure of these particles needs to be understood first. To be more precise, the quantized energy levels, denoted by the quantum number n, of (anti-)hydrogen atoms. The quantum number l was introduced through the Schrödinger equation to quantize the orbital angular momentum of the electron [4]. l is defined as $0 \leq l < n$. Next to the orbital angular momentum, the electron possesses an intrinsic angular moment giving it its magnetic moment. This angular moment is also referred to as 'spin' and is described by the quantum number s where for an electron and positron $s = \frac{1}{2}$ [4]. As a result, the quantum number j is introduced to describe the total angular momentum where $j = |l - s|$. However, not only electrons or positrons have a spin but also (anti-)proton particles with $s = \frac{1}{2}$. Therefore, to properly understand the structure of (anti-)hydrogen particles, an additional quantum number f is introduced where $f = j + \frac{1}{2}, j - \frac{1}{2}$ [4]. Due to these additional quantizations, each energy level n of (anti-)hydrogen particles is split into two so-called hyperfine levels [4]. These hyperfine levels describe the orientation of the magnetic dipoles of the electron/positron and proton/antiproton. For

hydrogen, the ground state hyperfine splitting is defined as

$$\triangle E_{HFS}(f=1) - \triangle E_{HFS}(f=0) \tag{7}$$

where for $l = 0$ states, the hyperfine energy shift is

$$\triangle E_{HFS} = \frac{m}{M}\alpha^4 mc^2 \frac{4\mu_p}{3n^3}\left[f(f+1) - \frac{3}{2}\right] \tag{8}$$

with μ_p the proton magnetic moment and M the proton mass [4].
The quantum number m_f, which describes the projection of the total angular momentum on an axis, divides each hyperfine state into $2f+1$ sublevels as $m_f = -f, -f+1, ..., 0, ...f-1, f$ [4]. By introducing an external static magnetic field B, this degeneracy is observed to be broken because of the interaction between the magnetic field and the hydrogen atom. This phenomenon is called the Zeeman effect, which can be determined using the Breit-Rabi equation

$$\triangle E_{n,f=j\pm\frac{1}{2},m_f} = -\frac{\triangle E_{HFS}}{4} - \mu_p m_f B \pm \frac{\triangle E_{HFS}}{2}\sqrt{1 + 2m_f x + x^2} \tag{9}$$

where $x \equiv \frac{B(\mu_e(n)+\mu_p)}{\triangle E_{HFS}}$, μ_e and μ_p are the magnetic moment of the electron and proton respectively [4].

Fig.5 shows the Breit-Rabi diagram of the energy levels of the ground state (anti-)hydrogen with respect to the strength of the external magnetic field B. The diagram depicts the splitting of the two zero B-field states into four non-zero B-field states, labeled $|a\rangle, |b\rangle, |c\rangle$ and $|d\rangle$ [7]. The states with a positive slope, here described by $|c\rangle$ and $|d\rangle$, are called low-field seekers. $|a\rangle$ and $|b\rangle$ states have a negative slope and are labeled as high-field seekers. Only low-field seeking states represent diamagnetic properties meaning that only atoms in these states may be trapped in a three-dimensional magnetic minimum [10] [11]. In the case where the B-field of a minimum accidentally goes to zero, a trapped (anti-)hydrogen atom can escape as a result by making a spin-flip transition to a high-field seeking state. These transitions are also referred to as Majorana transitions [12] [13].

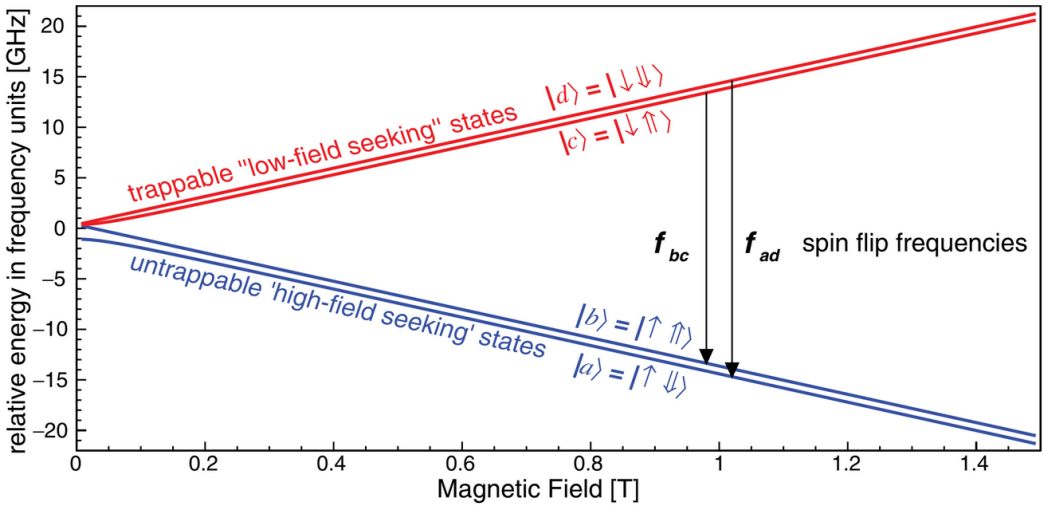

Figure 5: Breit rabi diagram of the energy level in the ground state (anti-)hydrogen as a function of the strength of an external magnetic field. Image from [7].

3 Design

All simulations and animations are modeled and run using the Comsol Multiphysics 6.0 (Classkit License) software. In this part, the different steps to obtain two promising models to construct a Ioffe trap, using only permanent magnets, are showcased. Important note, all the following geometrical dimensions for the different permanent magnets are only a suggestion by the author and can be alternated if needed during the possible construction phase of the underneath presented trap models.

3.1 Material

To be able to replicate the magnetic field of permanent magnets in Comsol accurately, a promising material should be used. For all the simulations, N52 (sintered NdFeB) magnets are selected. According to Comsol, the remanent flux density norm Br for this material is 1.44T. NdFeB, also known as neodymium magnet, is the most widely used type of rare-earth magnet, as it possesses a high Maximum Energy Product $(BH)_{max}$ [14]. The $(BH)_{max}$ is a major indicator of magnetic strength. It graphically describes the largest rectangle that can be drawn between the origin and the saturation demagnetization B-H curve, see Fig.. [15]. From all sintered NdFeB magnets, the N52 presents the highest Maximum Energy Product $(BH)_{max}$ of 50-53 MGOe (mega-gauss-oersted) or 398-422 $\frac{kJ}{m^3}$, thus being considered as the strongest commercially available neodymium magnet [14].

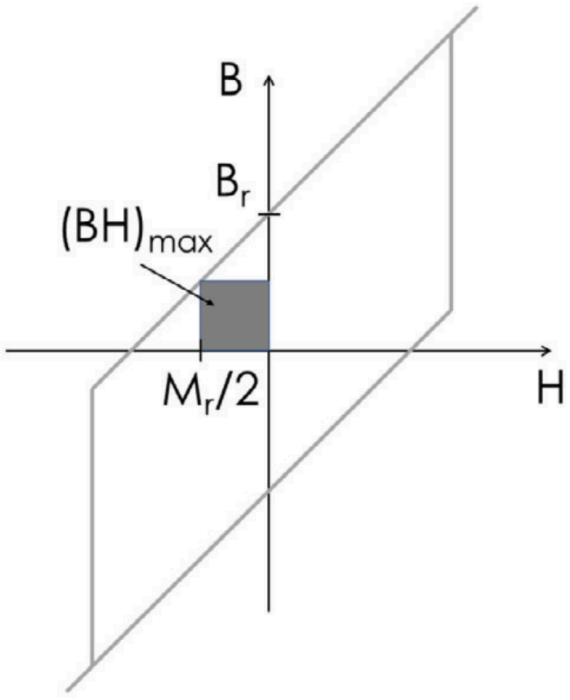

Figure 6: $B(H)$ Hysteresis loop of an ideal permanent magnet where $(BH)_{max}$ presents the largest rectangle which fits between the origin and $B-H$ curve. Images taken from [15]

3.2 Magnetic flux density study

3.2.1 Single Permanent Magnet

At first glance, the magnetic field created by a single permanent magnet behaves the same as the field created by an inductor. In both cases, the south pole describes the surface where the magnetic field lines enter and the north pole depicts the surface where the field lines exit. For an inductor, the magnetic field inside the inductor is homogeneous and all the field lines move from the S-pole to the N-pole. For a hollow permanent magnet, as seen in Fig.7, the field lines inside the magnet travel homogeneously from the N-pole to S-pole even though outside the permanent magnet the field lines still follow the conventional way. This observation might be interesting in regard to building potentially a penning trap using permanent magnets. Similar to a penning trap, there exists a homogeneous magnetic field for a hollow cylindrical magnet which potentially could trap charged particles. However, for this report, this is not further investigated.

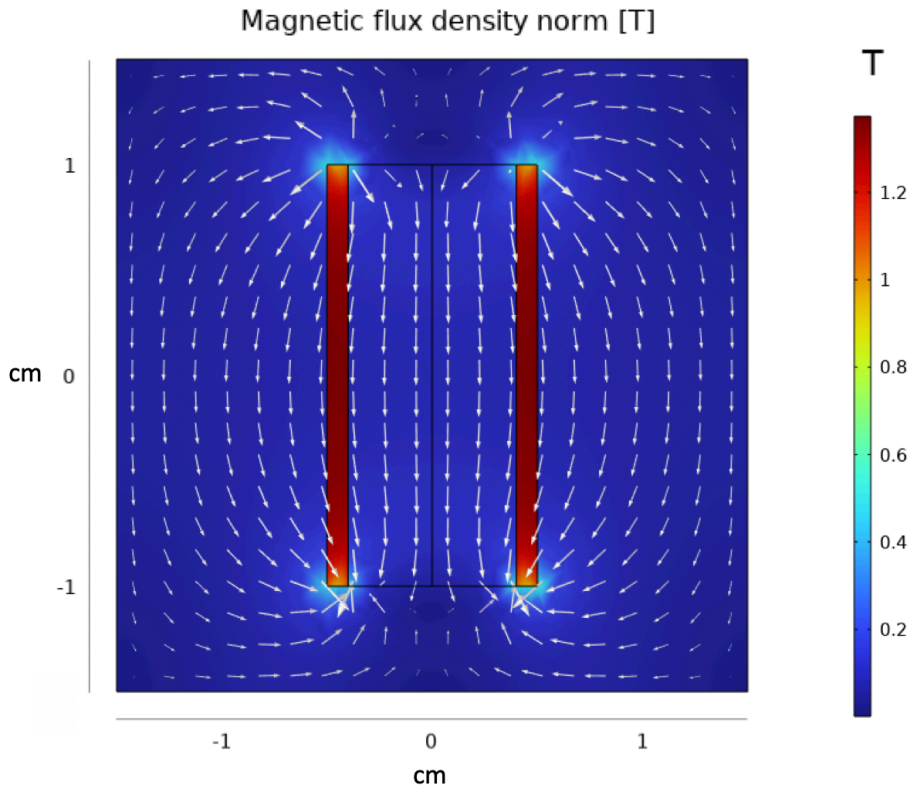

Figure 7: Magnetic field lines for a hollow cylindrical permanent magnet. The N-pole (top) and S-pole (bottom) are along the z-axis.

3.2.2 Quadrupole

As mentioned in section 2.2, an Ioffe trap is made of two parts, the quadrupole and the mirror coils.
Conventionally, the quadrupole is made of superconducting wires with opposite directions of current running in each wire.

To best replicate this configuration using permanent magnets, four rectangular magnets, of the same size, are aligned circularly around the axis of confinement. The dimensions of the permanent magnets used in Comsol are 5cm long and 1cm wide. The magnets are aligned in such a way that the two oppositely placed magnets face the same pole side. Meaning that in this case, the two magnets placed along the z-axis face each other's S-pole side and the two magnets placed along the x-axis their N-pole faces each other. The magnetic field lines should as a result imitate the field lines of a quadrupole using superconducting wires. This assumption is confirmed while doing a magnetic flux density norm study along the zy and zx planes. As shown in Fig.8a, a magnetic field minimum is observed along the trap axis, y-axis, thus creating an axially confined magnetic field. In addition, to the central magnetic field minimum, Fig.8b suggests that four other regions with a magnetic field minimum appear at the outer part of the quadrupole. These minima are due to the geometrical structure chosen and the resulting alignment of the field lines.

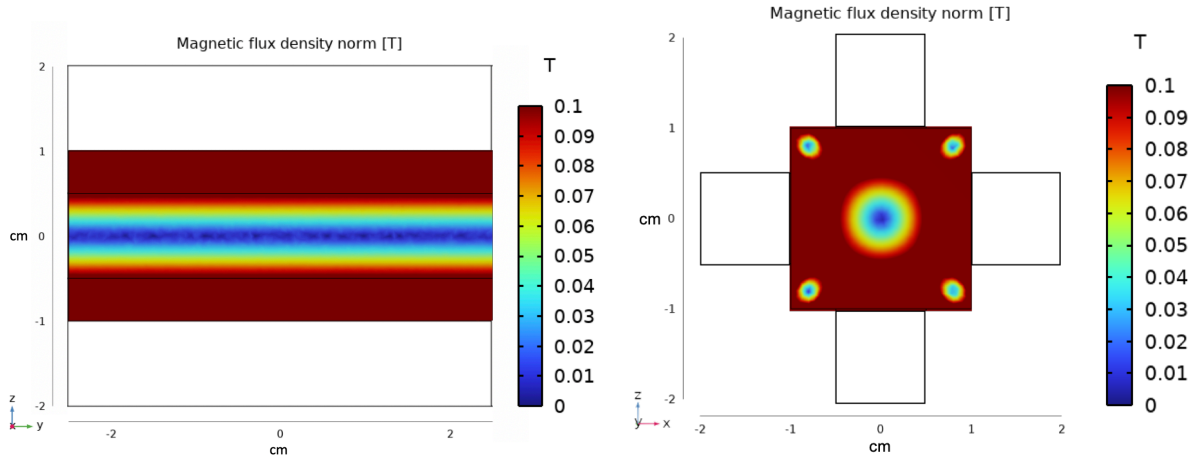

(a) (b)

Figure 8: (a) Magnetic flux density study of the quadrupole along the zy plane.(b) Magnetic flux density study of the quadrupole along the zx plane.

3.2.3 Ring magnets as mirror coils

The magnetic trap needs to be able to confine a particle radially. Conventionally, two mirror coils, current loops, with the same current direction produce a magnetic field that closes the trap on both sides. Intuitively, the use of ring magnets seems logical as they provide a similar shaped field as current loops. Fig.9 illustrates this idea of such a design. For a current loop, the electric field creates a magnetic field that concentrates in the center of the loop. For a ring magnet, the field lines enter from one end of the ring and rejoin from the other end creating thus the N and S-pole.

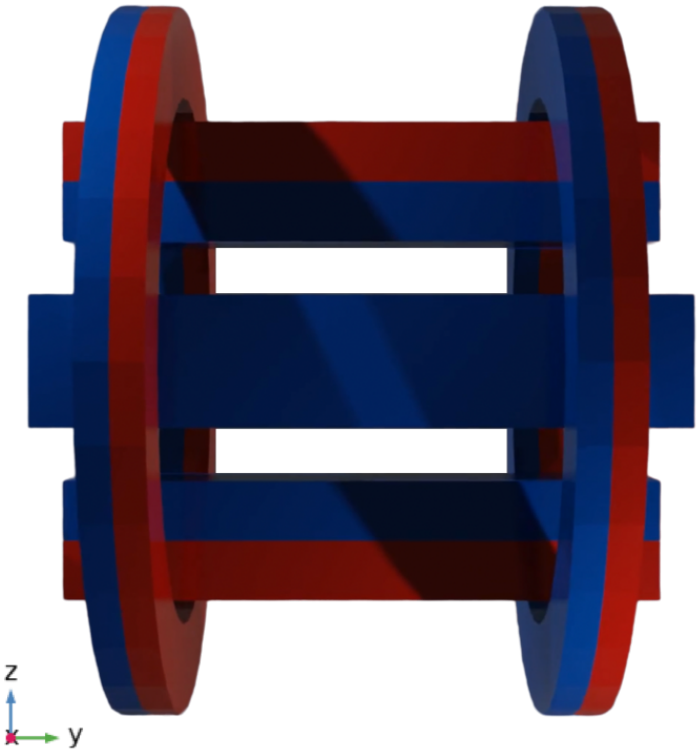

Figure 9: Illustration of the presented model where two identical ring magnets are used to replace the two mirror coils. The N-poles are coloured red and the S-poles are coloured blue. Illustration made in Blender software.

The used ring magnets are 0.25cm thick and 0.5cm long. To examine whether it is possible to create a sufficient radial B-field, by placing the two identical ring magnets at each end of the quadrupole, different configurations are examined. First, the ring magnets will be positioned 1cm inside the quadrupole, secondly, they will be moved at the end of the quadrupole and lastly, they will be moved outside of the trap. Fig.10a depicts the magnetic field flux density, in the zy plane, for the case where the ring magnets are placed inside the quadrupole magnets. To better determine whether a confined minimal field is created, the illustrated B-field strength is limited to 0.05T. From Fig.10a, it is suggested that a small confined central magnetic field is created. However, as it is not completely obvious, an isosurface study is done for 0.02T which is shown in Fig.10b. An isosurface study enables to represent the magnetic field three-dimensionally. Using Fig.10b it is proven that there exists a magnetic minimum in the center of the trap at low B-field strengths. The next step is to identify the axis where the registered B-field depth is the smallest. In this case, it is along the trap axis, the y-axis. Fig.11 depicts the magnetic flux density norm along the y-axis for all three different cases. Using equation 4, the trap depth values are determined as a result. It is noticed that the smallest trap depth value, 0.009K, is associated with the case where the ring magnets are placed inside the quadrupole. The highest predicted value is for the case where the magnets are outside the quadrupole magnets with 0.013K. However, this value is very small compared to the 0.38K and 0.54K trap depth values for the Ioffe traps used at ATRAP and ALPHA respectively [2][3].

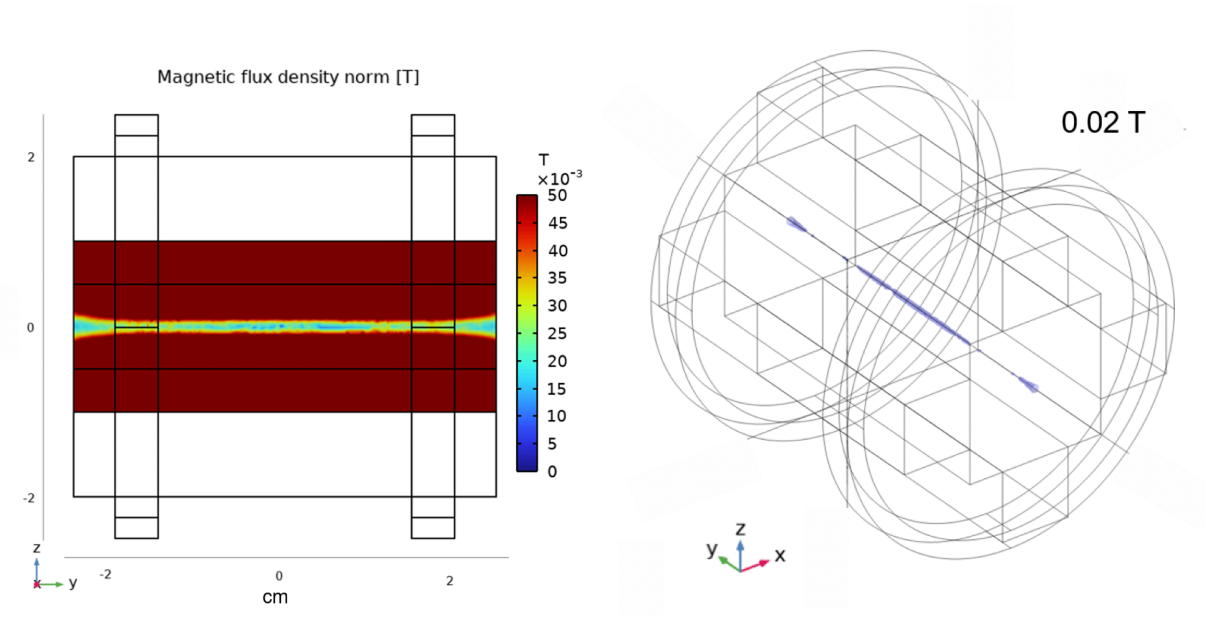

(a) (b)

Figure 10: (a) Magnetic flux density study of the model using small ring magnets, along the zy plane.(b) Isosurface at 0.02T for the model using small ring magnets.

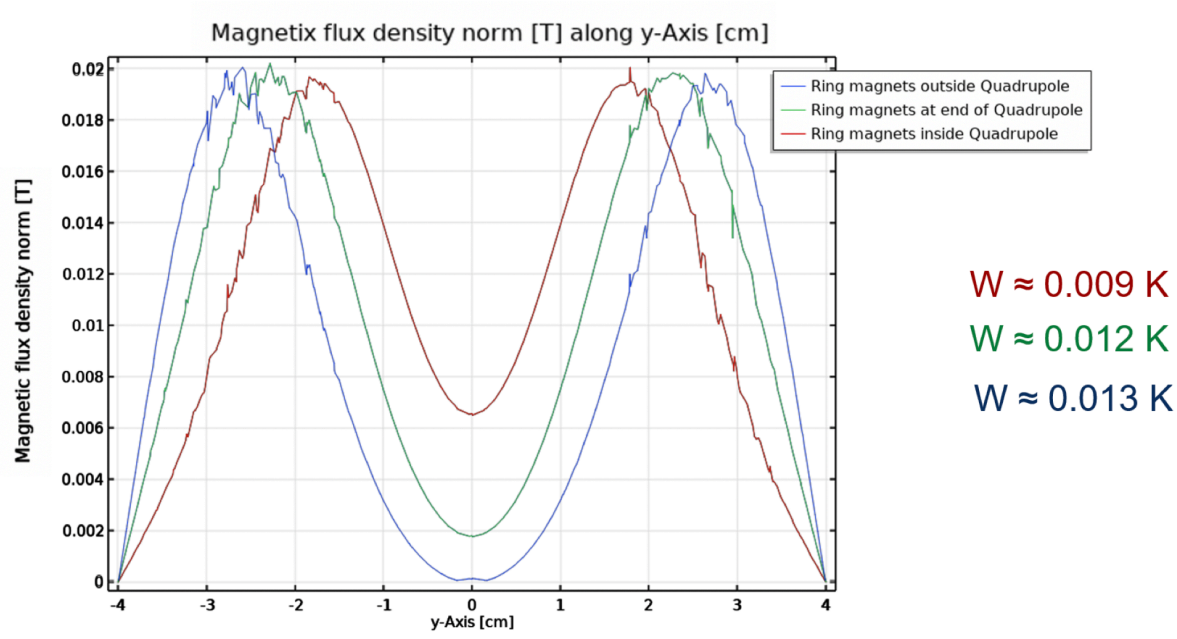

Figure 11: Magnetic flux density norm study along the y-axis for (blue) when ring magnets are outside quadrupole. (green) when ring magnets are at the end of the quadrupole. (red) when ring magnets are inside the quadrupole.

Thus, to increase the trap depth value, the magnetic field of the ring magnets need to increase. This is achieved by introducing 1.75cm thick and 0.5cm long ring magnets. Fig.12a and Fig.12b

represent the magnetic flux density norm in the zy plane and the isosurface at 0.1T respectively. Both figures suggest that an improved radial confinement is possible as a confined non-zero B-field minimum is noticeable at the center of the trap. Using Fig.13, the field strength along the y-axis for all three cases is investigated. This time, it is also noticeable, that the confined magnetic minimum is the most noticeable for the case where the ring magnets are introduced outside of the quadrupole magnets with the highest observed trap depth value being 0.04K. It can be concluded that by increasing the size of the ring magnets, the resulting trap depth increased but in the end is still considered to be too small. Due to the fact that the strength of a permanent magnet is limited, it suggests that the ring magnets need to become even more wider and thicker in the hope of getting a promising trap depth. This suggests that there might be other more interesting configuration to investigate which could promise a more convincing result.

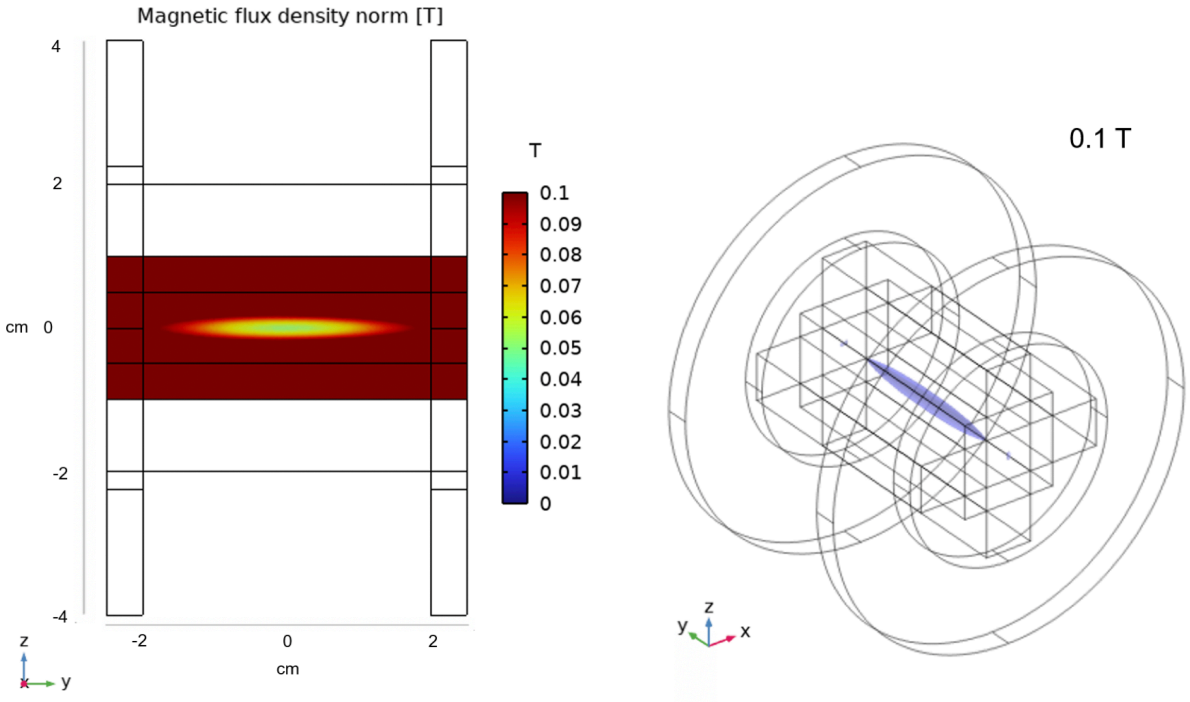

(a) (b)

Figure 12: (a) Magnetic flux density study of the model using bigger ring magnets, along the zy plane.(b) Isosurface at 0.1T for the model using bigger ring magnets.

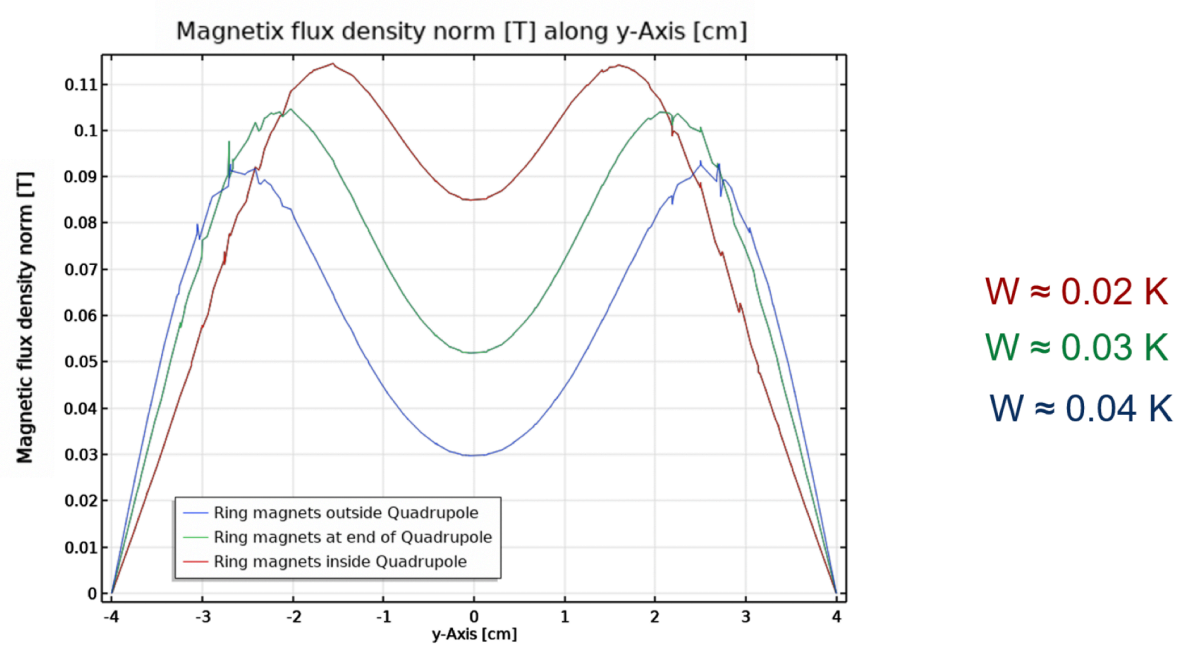

Figure 13: Magnetic flux density norm study along the y-axis for (blue) when the bigger ring magnets are outside quadrupole. (green) at the end of the quadrupole. (red) inside the quadrupole.

3.2.4 Changing shape of Quadrupole

Another idea to possibly trap particles radially is to alternate the shape of the magnets that constitute the quadrupole. Meaning that the magnets should have a maximal magnetic field at their ends. In order to achieve such a magnetic field, it would be plausible to introduce, on each side of the quadrupole magnets, another set of permanent magnets. The dimensions of these magnets can vary but in this case, 1cm long and 1.5cm thick magnets are used. As previously mentioned, in order to create a trapping magnetic field radially, each end of the quadrupole magnets needs to create a B-field of opposite direction. Thus, suggesting that all the additional magnets on one end of the quadrupole need to have their N-side facing towards the trap axis, here the y-axis, and all the magnets used on the other side of the quadrupole need to face their S-pole towards the trap axis. This is best illustrated in Fig.14.
When studying the magnetic flux density norm along the zy plane of this model in Comsol, a confined magnetic minimum is noticeable at the center of the trap, as shown in Fig.15a. Fig.15b represents an isosurface of the field at 0.17T. It is observed that next to the central magnetic minimum, the field creates two additional minima on each end. These small minima are a result of the magnetic field lines that interact between the quadrupole magnets and the additional magnet pieces. Fig.16, suggests that the smallest magnetic field difference between the center and walls of the trap would occur along the trap axis, the y-axis. Resulting in a suggested trap depth of 0.25 K. However, as it was noticed previously in section 3.2.2 when investigating the B-field of a quadrupole, there appear to be four other magnetic minima along the outer radius of the trap. As a result, when investigating the magnetic field diagonally along the trap, using Fig.17b, it is observed that the magnetic field strength difference is smaller along the y-axis as shown in Fig.17a. Meaning that the trap depth is 0.21 K. This implies that (anti-)hydrogen

Figure 14: Illustration of the second presented model, where the shape of the quadrupole magnets is alternated. The N-poles are colored red and the S-poles are coloured blue. Illustration made in Blender software.

particles could escape the central B-field minimum diagonally, which is the most likely. Thus making the diagonal axis the weak point of this model. Even in that worst-case scenario, the trap depth is significantly greater than for the previous model, suggesting that it could potentially trap particles with kinetic energy up to 0.21 K.

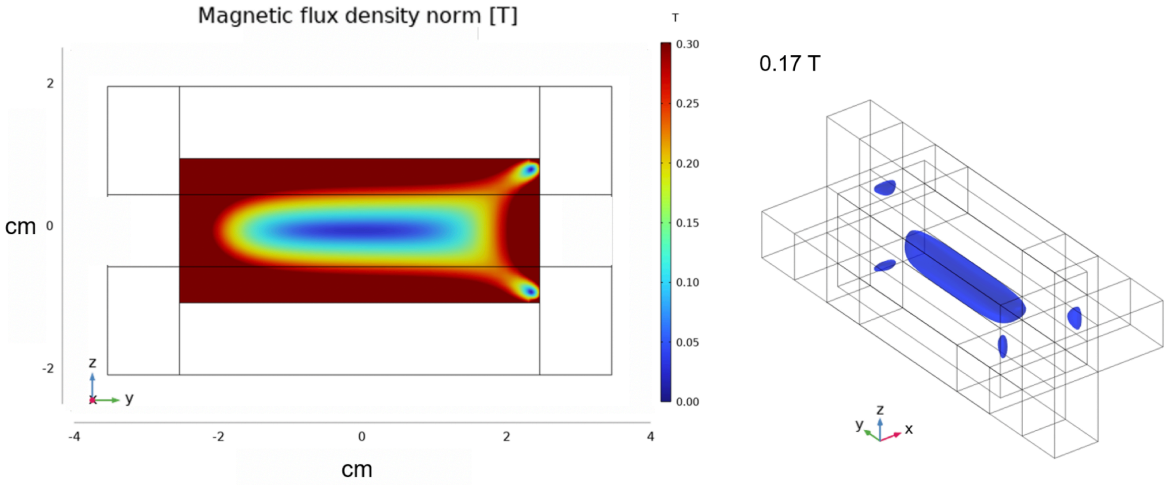

(a) (b)

Figure 15: (a) Magnetic flux density for the design of an Ioffe trap where the shape of the quadrupole magnets is changed. (b) Isosurface at 0.17T.

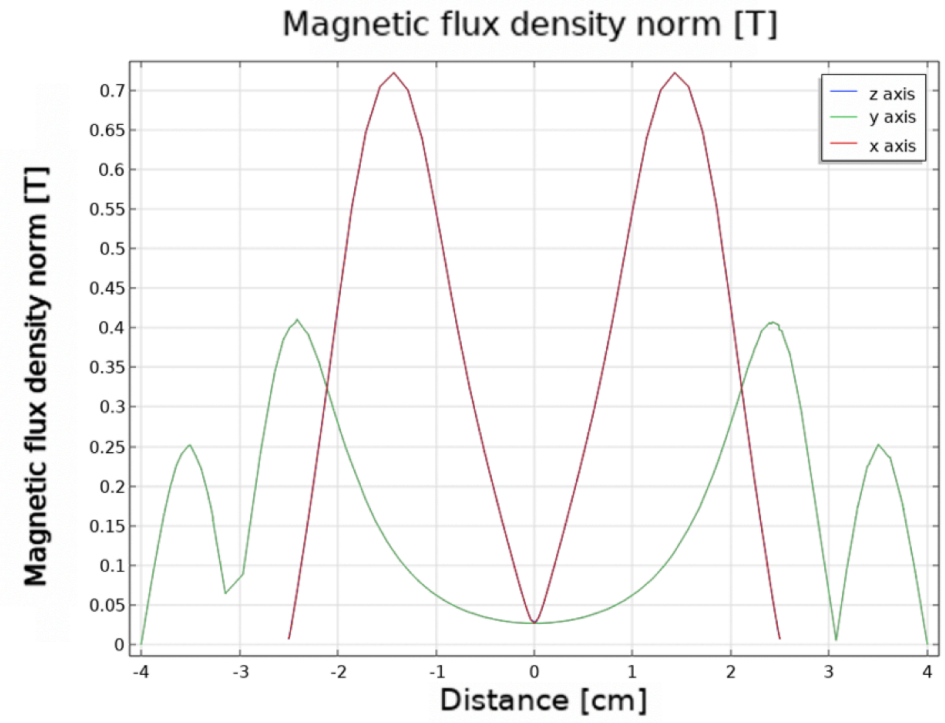

Figure 16: Magnetic flux density study along the x,y and z axes. It is observed that along the y-axis the B-field depth is the smallest. It is also noticed that the magnetic field along the x and z axes is the same.

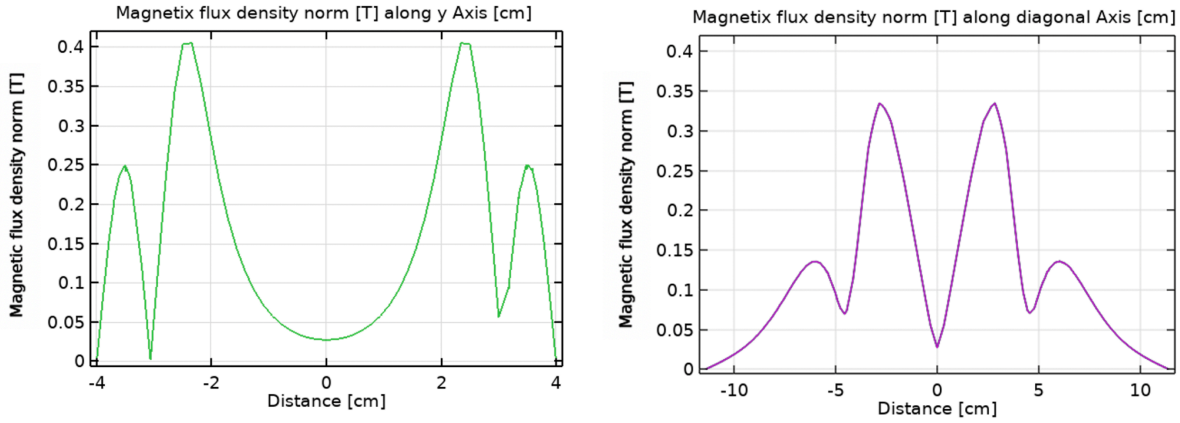

(a) (b)

Figure 17: (a) Magnetic flux density study along the y-axis.(b) Magnetic flux density study along the diagonal axis.

To fully confirm whether this presented model could potentially trap (anti-)hydrogen atoms, a neutral particle of mass similar to the proton mass is introduced in the center of the trap. Using Comsol, simulations are conducted with different kinetic energies for the particle. For each

simulation, the neutral particle is released along the diagonal axis of the trap. It is interesting to investigate the case where the particle would present a kinetic energy slightly higher than the determined trap depth of the trap. Fig.18 presents the particle trajectory for a particle with a kinetic energy of 0.24K. At the beginning, the particle oscillates along the trap axis, inside the central magnetic minimum. When reaching the end of the trap, the particle bounces back and starts to travel back. Initially, the particle moves mostly in the xy plane before starting to oscillate more constantly in the zy plane. At this point, the particle seems to be trapped. However, after a short time, the particle deviates from its trajectory and ends up leaving the trap diagonally. This confirms the observation that for this model, a particle with a high enough energy is most likely to escape diagonally. Fig.19 describes the trajectory of a particle that has a kinetic energy of 0.22 K and represents the upper limit for the kinetic energy where theoretically a particle is able to be trapped. In this case, it can be observed that even though the particle moves quite dynamically inside the magnetic minimum that it does not collide with the walls or escapes the trap over a measured time of 10 ms. It could be that when running the simulations for a longer time that the particle might escape after a time due to the fact that it has a high kinetic energy. In this specific case, the particle is classified to be quasi-trapped. However, by showing that it stays trapped for at least 10 ms, it is proven that the calculated trap depth is promising.

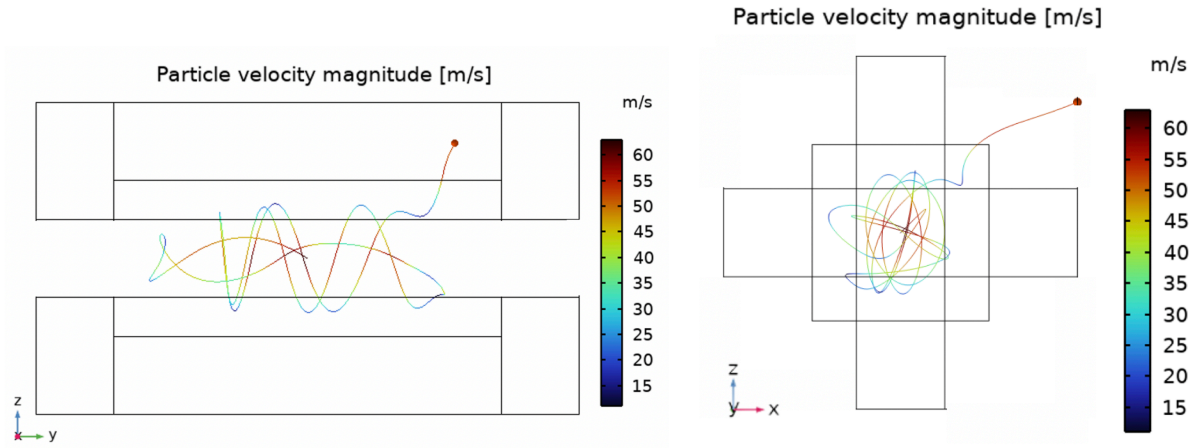

(a) (b)

Figure 18: Trajectory of a neutral particle with mass equivalent to proton mass and kinetic energy of 0.24K along (a) the zy plane. (b) the zx plane. The particle escapes the trap diagonally.

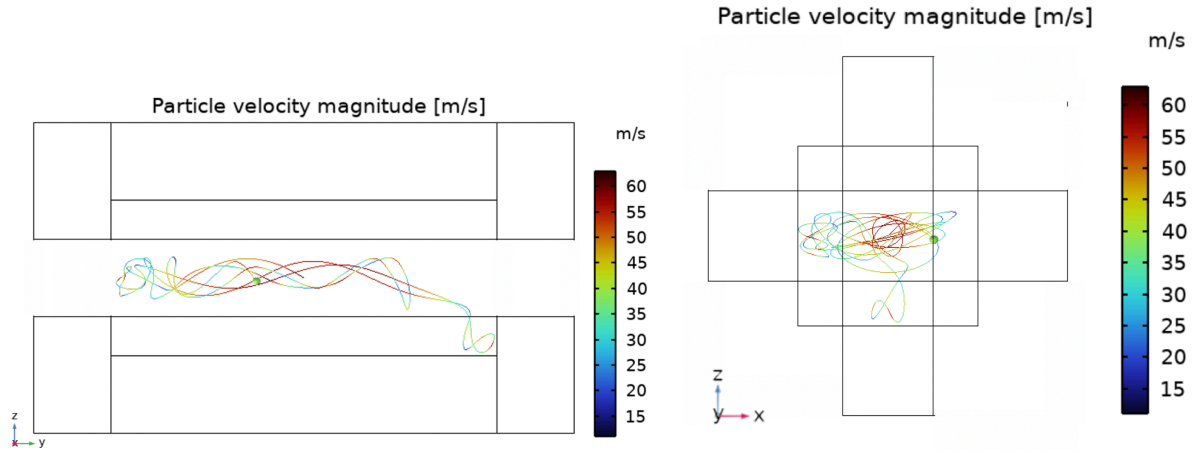

(a) (b)

Figure 19: Trajectory of a neutral particle with mass equivalent to proton mass and kinetic energy of 0.22K along (a) the zy plane. (b) the zx plane. The particle stays trapped over a time of 10ms.

3.2.5 Closing the trap using permanent magnets

Even though the previously mentioned model presented promising results for trapping (anti-)hydrogen particles, it would be interesting to investigate a model where it will not be necessary to change the geometry of the quadrupole magnets, thus reducing the number of additional magnet pieces needed. The idea is to replace the mirror coils with small quadratic magnets along the trap axis. As for the other models, the geometrical dimension used are only suggestions. The two 'closing' permanent magnets used in these simulations are 1cm long and 1cm thick. In order to introduce particles inside the trap, the magnets will have a central hole of 0.1cm radius. The two 'closing' magnets will be aligned along the trap axis, each on one end of the quadrupole. As depicted in Fig.20, the N-pole side of one of the magnets will face towards the center of the trap and for the other permanent magnet, it will be its S-pole side. Both closing magnets are positioned exactly outside of the quadrupole along the trap axis due to the result obtained in section 3.2.3.

Fig.21a shows the magnetic flux density norm for this model along the zy plane. The resulting plot is similar to the result of the previous model. Meaning, that there is a visible central magnetic minimum inside the trap. When looking at the isosurface plot, Fig.21b, for 0.14T, the resemblance is even more clear. Also in this case, two small B-field minima occur at each end of the central minimum. When investigating the magnetic flux density along each primal axis, x,y and z, in Fig.22, it is again observed that the y-axis represents the smallest magnetic field strength difference. Comparing the field density along the y-axis with the diagonal axis using Fig.23 , it is noticeable that both axes have almost the same B-field depth. This indicates that for this model, the diagonal and trap axes are the weak points. Nonetheless, the calculated trap depth happens to be the same as for the previous model, at 0.21 K.

Figure 20: Illustration of the third presented model, where on each side of the quadrupole a 'closing' magnet is introduced. The N-poles are coloured red and the S-poles are coloured blue. Illustration made in Blender software.

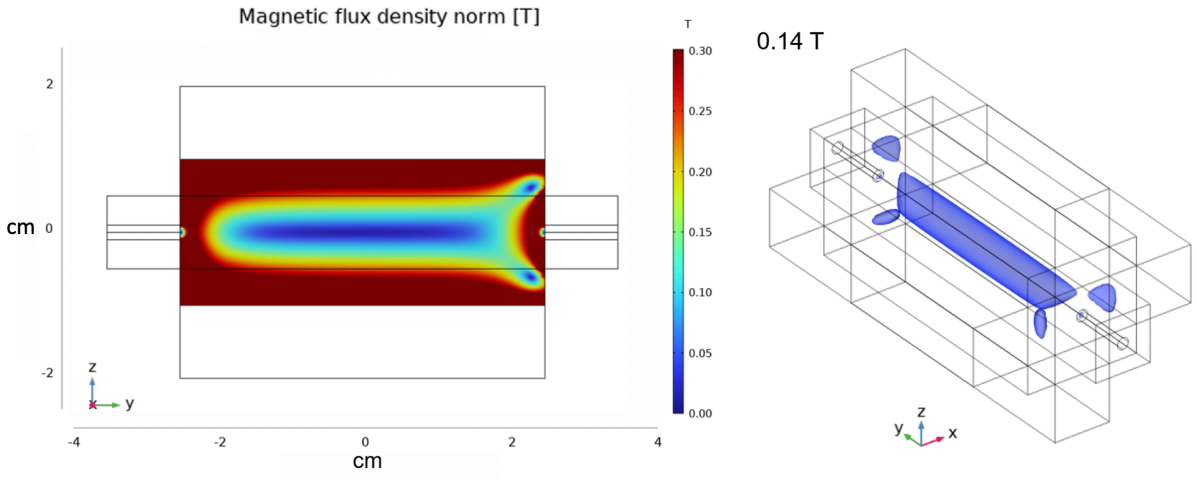

(a) (b)

Figure 21: (a) Magnetic flux density for the design of an Ioffe trap where two cube magnets are used to close the trap radially. (b) Isosurface at 0.14T.

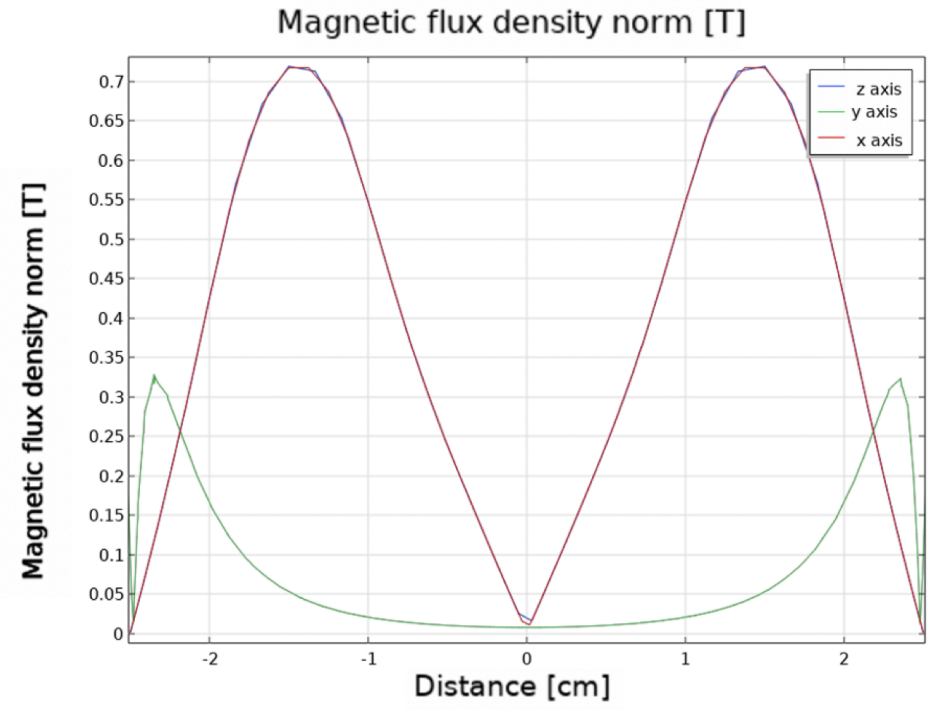

Figure 22: Magnetic flux density study along the x,y and z axes. It is observed that along the y-axis the B-field depth is the smallest. It is also noticed that the magnetic field along the x and z axes is the same.

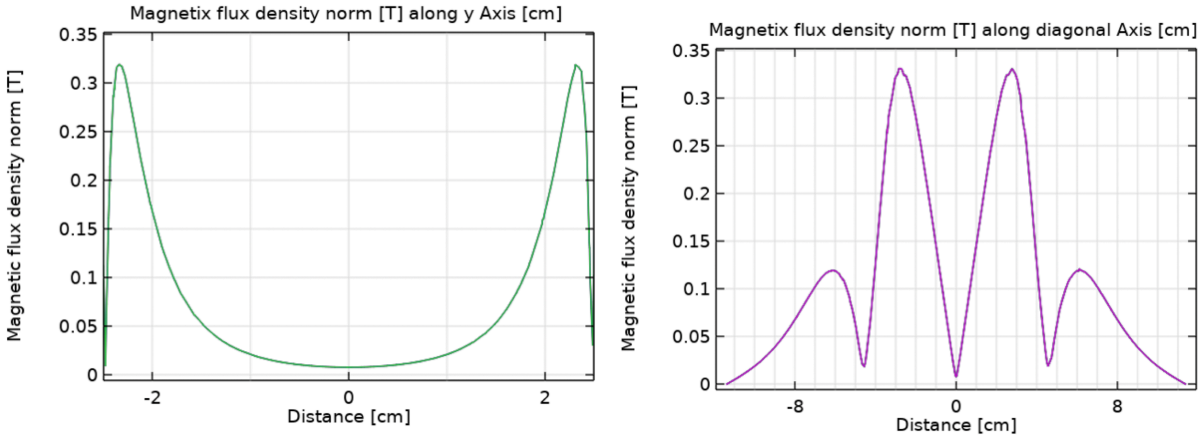

(a) (b)

Figure 23: (a) Magnetic flux density study along the y-axis. (b) Magnetic flux density study along the diagonal axis.

In the same way as in the previous subsection 3.2.4, a neutral particle with the mass of a proton is placed at the center of the trap and is given different kinetic energies. The particle is positioned in such a way that it will move diagonally at the beginning. First of all, the particle

is given a kinetic energy of 0.24K which is a bit higher than the theoretical trap depth value of 0.21K. The resulting particle trajectory, shown in Fig.24, is similar to the result from the model discussed in section 3.2.4. Meaning that the particle first oscillates along the zy plane before drifting slowly towards the zx plane and leaving the trap diagonally. When giving the particle a kinetic energy of 0.22K, the particle shows first signs of staying confined in the central magnetic minimum, which is shown in Fig.25. These simulations confirm the possibility that this design could also potentially trap (anti-)hydrogen particles.

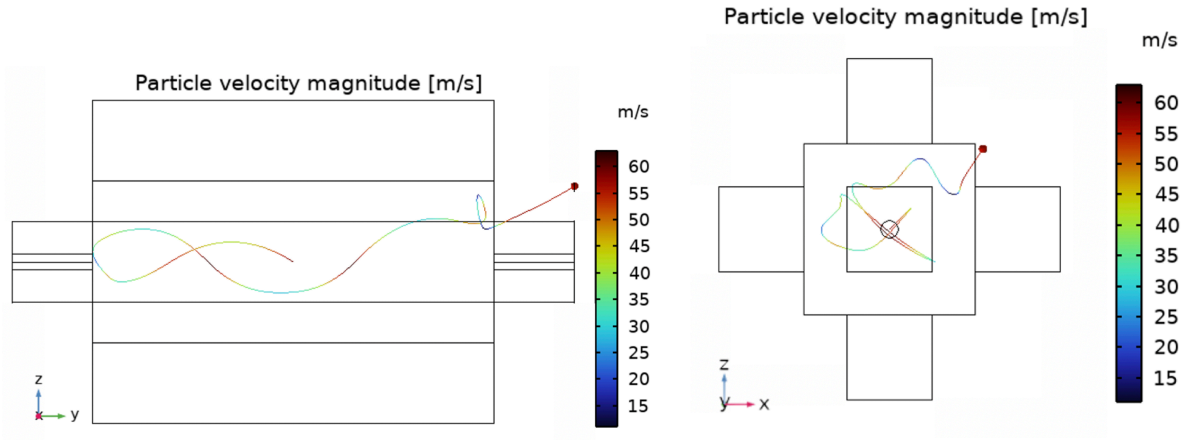

(a) (b)

Figure 24: Trajectory of a neutral particle with mass equivalent to proton mass and kinetic energy of 0.24K along (a) the zy plane. (b) the zx plane. The particle escapes the trap diagonally.

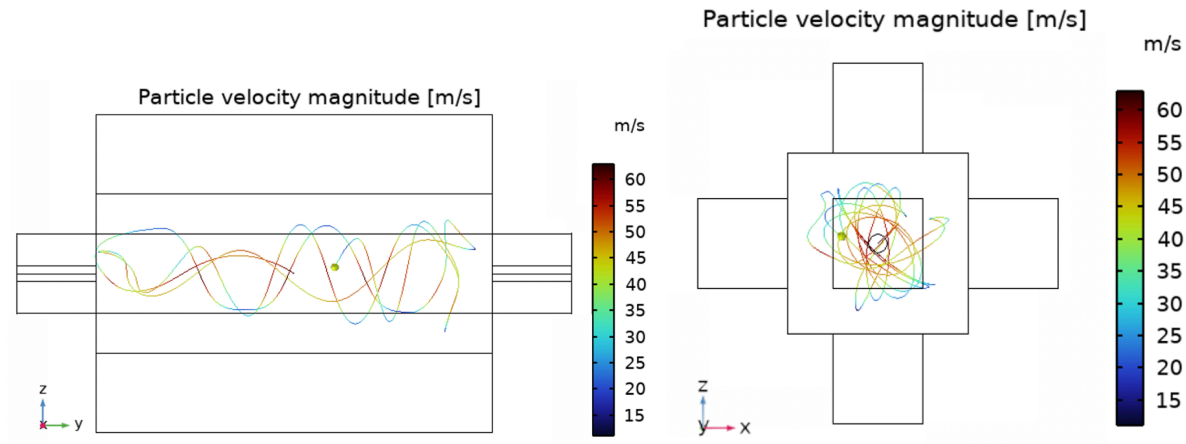

(a) (b)

Figure 25: Trajectory of a neutral particle with mass equivalent to proton mass and a kinetic energy of 0.22K along (a) the zy plane. (b) the zx plane. The particle stays trapped over a time of 10ms.

4 Discussion

Three possible designs for an Ioffe trap, using N52 (sintered NdFeB) magnets, were discussed in this report under section 3.
Replicating the magnetic field of a quadrupole using four permanent magnets resulted in success. By placing the magnets circularly around the axis of confinement, where oppositely positioned magnets face the same pole side to each other, resulted in a two-dimensional confined field. To confine the field radially, three different designs were presented. In the first model, ring magnets are used. In the second, the field of the quadrupole magnets is alternated by adding additional permanent magnet pieces on each end of the quadrupole magnets. Lastly, on each end of the trap, a quadratic magnet with a small hole, is placed along the trap axis.
After studying the magnetic flux density, it is shown that it is possible to create a three-dimensional magnetic minimum inside the trap, for all three models. Between the three models, there are some differences observed.

Even though the first model is a geometrical replication of a conventional Ioffe trap, only replacing the superconducting wires with permanent magnets, it shows the least promising results. The highest determined trap depth value is around 0.04K. To put things in perspective, the observed trap depth values at the ALPHA and ATRAP experiments are 0.54K and 0.38K, respectively. This value is negligible as the trap depth value represents the theoretical maximum kinetic energy a (anti-)hydrogen particle can have to stay trapped inside the trap. Meaning that a lower value indicates fewer particles are trapped. For this design, along the trap axis, here the y-axis, the smallest B-field depth is observed. Therefore, representing the weak point axis of the model. Another disadvantage is observed while rescaling the size of the closing ring magnets. By rescaling the ring width from 0.25cm to 1.75cm, the trap depth value only increased from 0.013K to 0.04K. Even though, the radial magnetic field increased, it is not significant enough to obtain a promising trap depth. Suggesting that this model will not provide an attractive alternative to conventional (anti-)hydrogen traps.
The trap depth value obtained for the second design model is calculated to be 0.21K. The observed magnetic central minimum is more promising, as a result, compared to the first model. It is observed that due to the quadrupole configurations, two minima occur on each end of the trap along the trap axis. This is a result of the interaction between the magnetic field lines between the quadrupole magnets and the additional magnets. In this case, it is observed that the minimal field depth is along the diagonal axis of the trap. This is confirmed by running simulations, which show that particles escape the trap diagonally when they are provided with a kinetic energy higher than 0.22K. When providing these particles with energies comparable to the trap depth value, they are observed to be trapped over a period of time, here 10ms. As a result, this model presents promising results.
For the third model, the trap depth value is also observed to be around 0.21K. As a result, the magnetic minimum is similar to the results presented for the second model. The only difference is that for this model, the smallest observed B-field depth is very similar along the trap axis, the y-axis, and the diagonal axis. The simulations give the same results as for the other model. In cases, where a particle possesses kinetic energy higher than the trap depth value, it escapes. Otherwise, it seems to stay trapped.
All in all, it can be concluded that only the second and third presented models depict promising results, which could encourage the development of building Ioffe traps out of permanent magnets.

After proving that it is theoretically possible to build an Ioffe trap using only permanent magnets, its advantages and limitations compared to conventional (anti-)hydrogen traps need to be discussed.
The most striking disadvantage is the static magnetic field of a permanent magnet. Superconducting wires create a magnetic field depending on the current that travels through them. Thus, by changing the provided current intensity, the strength of the magnetic field can also be changed. This has the advantage that the Ioffe trap could be 'switched off' in case of an emergency by lowering the current intensity. In addition, the strength of the magnetic field, created using superconducting wires, can exceed the upper B-field limit of permanent magnets. As a result, traps with higher trap depth values are produced which consequently trap more (anti-)hydrogen particles inside. To recall, the strongest commercially available permanent magnets to date are N52 neodymium magnets which have a maximum residual magnetic flux density of 1.44T. The maximum trap depth value observed by the models presented in this report is 0.21K which is smaller than the 0.54K value observed at the ALPHA experiment.
On the other hand, financially, it is more attractive to switch to Ioffe traps made of permanent magnets. The biggest disadvantage of conventional Ioffe traps is that they need to be cryogenically cooled, using for example Helium, as they can only operate at very low temperatures, around 4K. As a result, high maintenance costs significantly increase the price of the experiment, so only big budget institutes are available to acquire them. Permanent magnets, being relatively cheap, don't need to be cooled, minimising building and maintenance costs. As a result, making fundamental research more accessible.

5 Conclusion

In this report, three different designs for a potential Ioffe trap, build exclusively out of N52 neodymium magnets, are presented. All three designs show that it is possible to create a non-zero three dimensional magnetic minimum at their center. However, for the first presented model, where ring magnets are used to radially close the trap, the maximal resulting trap depth value is only 0.04K. As this value is an order of 10 smaller than what conventional Ioffe traps provide, it suggest that this approach is not of interest. For both other models, the trap depth is found to be around 0.21K. When studying the magnetic flux density inside the traps, it is observed that for the second model, the diagonal axis represents the weakpoint. For the third model, a particle is mostly likely to escape along the trap and diagonal axis. Nonetheless, both models provide similar results by being able to trap (anti-)hydrogen particles which have a kinetic energy up to the trap depth value. This confirms the research question of this report that it might be possible to create Ioffe traps based on only permanent magnets in order to trap (anti-)hydrogen particles. Due to the fact that the field strength of magnets can not be alternated compared to superconducting wires, the trap depth is limited and it is not possible to 'switch off' the trap in case of emergency. However, due to the fact that the trap does not need to operate at low temperatures, it is financial attractive alternative. Making it more accessible for research groups with limited budget to conduct fundamental research.

6 Outlook

This report managed to confirm that it is possible to design an Ioffe trap, made out of permanent magnets, based on theoretical and computational approaches. The next step would be to try and build such a trap in real life, which goes over the premise of this report. The most challenging part will be placing all the neodymium magnets next to each other. As a result, a quick force study, using COMSOL, is conducted. The results are only based on approximations and thus only provide estimations. Nonetheless, it is predicted that between the magnets, forces of the order of 100N would exist.

7 Bibliographie

[1] S. A. Jones, "An ion trap source of cold atomic hydrogen via photodissociation of the bah+ molecular ion," *New Journal of Physics*, vol. 24, no. 2, p. 023 016, Feb. 2022. DOI: 10.1088/1367-2630/ac4ef3. [Online]. Available: https://dx.doi.org/10.1088/1367-2630/ac4ef3.

[2] C. Amole, M. Ashkezari, M. Baquero-Ruiz, *et al.*, "An experimental limit on the charge of antihydrogen," *Nature Communications*, vol. 5, 2014. DOI: https://doi.org/10.1038/ncomms4955.

[3] E. Tardiff, X. Fan, G. Gabrielse, *et al.*, "Two-symmetry penning-ioffe trap for antihydrogen cooling and spectroscopy," *Nuclear Instruments and Methods in Physics Research Section A: Accelerators, Spectrometers, Detectors and Associated Equipment*, vol. 977, p. 164 279, 2020, ISSN: 0168-9002. DOI: https://doi.org/10.1016/j.nima.2020.164279. [Online]. Available: https://www.sciencedirect.com/science/article/pii/S0168900220306756.

[4] S. A. Jones, "Observation of the 1s-2s transition in trapped antihydrogen," 2017. [Online]. Available: https://alpha.web.cern.ch/sites/default/files/2020-05/Full%20thesis%2010.pdf.

[5] G. B. Andresen, M. D. Ashkezari, M. Baquero-Ruiz, *et al.*, "Trapped antihydrogen," *Nature*, vol. 468, no. 7324, pp. 673–676, Dec. 2010.

[6] C. A. science. "Manipulation of antiprotons, positrons and other charged particles - ioffe-pritchard trap." (2023), [Online]. Available: https://alpha.web.cern.ch/science/ioffe-pritchard-trap (visited on 05/17/2023).

[7] R. C. T. M. Knoop N. Madsen, *Advanced Textbooks in Physics Trapped Charged Particles, A Graduate Textbook with Problems and Solutions*. World Scientific, 2016.

[8] M. Vogel, *Particle Confinement in Penning Traps, An Introduction*. Springer, 2018.

[9] S. P. Benz, A. Pollarolo, J. Qu, *et al.*, "An electronic measurement of the boltzmann constant," *Metrologia*, vol. 48, no. 3, p. 142, Mar. 2011. DOI: 10.1088/0026-1394/48/3/008. [Online]. Available: https://dx.doi.org/10.1088/0026-1394/48/3/008.

[10] W. Bertsche, A. Boston, P. Bowe, *et al.*, "A magnetic trap for antihydrogen confinement," *Nuclear Instruments and Methods in Physics Research Section A: Accelerators, Spectrometers, Detectors and Associated Equipment*, vol. 566, no. 2, pp. 746–756, 2006, ISSN: 0168-9002. DOI: https://doi.org/10.1016/j.nima.2006.07.012. [Online]. Available: https://www.sciencedirect.com/science/article/pii/S0168900206012617.

[11] M. Diermaier, C. B. Jepsen, B. Kolbinger, *et al.*, "In-beam measurement of the hydrogen hyperfine splitting and prospects for antihydrogen spectroscopy," *Nature Communications*, vol. 8, no. 1, p. 15 749, Jun. 2017. DOI: 10.1038/ncomms15749.

[12] D. M. Brink and C. V. Sukumar, "Majorana spin-flip transitions in a magnetic trap," *Phys. Rev. A*, vol. 74, p. 035 401, 3 Sep. 2006. DOI: 10.1103/PhysRevA.74.035401. [Online]. Available: https://link.aps.org/doi/10.1103/PhysRevA.74.035401.

[13] M. A. Alarcón, C. J. Riggert, and F. Robicheaux, "Simulations of majorana spin flips in an antihydrogen trap," *Journal of Physics B: Atomic, Molecular and Optical Physics*, vol. 52, no. 15, p. 155 004, Jul. 2019. DOI: 10.1088/1361-6455/ab29aa. [Online]. Available: https://dx.doi.org/10.1088/1361-6455/ab29aa.

[14] N. Hiron, A. Andang, and N. Busaeri, "Investigation of ndfeb n52 magnet field as advanced material at air gap of axial electrical generator," *IOP Conference Series: Materials Science and Engineering*, vol. 550, no. 1, p. 012 034, Jul. 2019. DOI: 10.1088/1757-899X/550/1/012034. [Online]. Available: https://dx.doi.org/10.1088/1757-899X/550/1/012034.

[15] J. Fischbacher, A. Kovacs, M. Gusenbauer, *et al.*, "Micromagnetics of rare-earth efficient permanent magnets," *Journal of Physics D: Applied Physics*, vol. 51, no. 19, p. 193 002, Apr. 2018. DOI: 10.1088/1361-6463/aab7d1. [Online]. Available: https://dx.doi.org/10.1088/1361-6463/aab7d1.